Available online at www.sciencedirect.com
SCIENCE DIRECT®
ELSEVIER
Ultramicroscopy 103 (2005) 199–204
ultramicroscopy
www.elsevier.com/locate/ultramic

Nondestructive three-dimensional characterization of grain boundaries by X-ray crystal microscopy

Wenjun Liu[a,*,1], Gene E. Ice[a], Bennett C. Larson[b], Wenge Yang[b], Jonathan Z. Tischler[b]

[a]*Metals and Ceramics Division, Oak Ridge National Laboratory, P.O. Box 2008, MS6118, Oak Ridge, TN 37831, USA*
[b]*Condensed Matter Sciences Division, Oak Ridge National Laboratory, P.O. Box 2008, MS6030, Oak Ridge, TN 37831, USA*

Received 12 July 2004; received in revised form 17 November 2004; accepted 22 November 2004

Abstract

The results from an emerging method of nondestructive grain boundary characterization, with unprecedented sensitivity to neighbor-grain misorientation and grain boundary morphology are reported. The method utilizes differential aperture X-ray microscopy to determine the local crystallographic orientation of submicron volumes within polycrystalline materials. Initial measurements are described for a recrystallized Ni sample where the grain boundary type was identified at 85 grain boundaries within the framework of an ideal coincident site lattice (CSL) model. The remarkable resolution of this method is demonstrated by the $<0.03^\circ$ deviations of misorientation measured for $\Sigma 3$ (twin) boundaries. Because of its high angular and spatial resolution, this new approach to grain boundary characterization can provide quantitative tests of grain boundary models with new insights for grain boundary engineering efforts.
Published by Elsevier B.V.

PACS: 61.10.yh; 61.72.mm

Keywords: 3d X-ray crystal microscopy; Grain boundary characterization; Coincident site lattice

1. Introduction

Grain boundaries are most often categorized according to a geometrical construction that assumes local minima in the grain boundary energy when some of the lattice sites from one lattice are coincident with some of the lattice sites from the neighbor grain. The so-called coincidence

*Corresponding author. Tel.: +1 630 252 0890; fax: +1 630 252 0862.
E-mail address: wjliu@anl.gov (W. Liu).
[1]Present address: UNI-CAT, Bldg 438D, Advanced Photon Source, Argonne National Laboratory, 9700 South Cass Avenue, Argonne, IL 60439, USA.

0304-3991/$ - see front matter Published by Elsevier B.V.
doi:10.1016/j.ultramic.2004.11.022

site lattice (CSL) model has become a cornerstone of grain-boundary structure research, particularly in materials of cubic system [1,2]. A boundary with a high density of coincident lattice points implies 'good fit' of adjacent grains with a modification of properties such as diffusivity, energy, and mobility. The Σ number of the coincident site lattice denotes the fraction of lattice sites that are in coincidence, e.g. $\Sigma 3$ means $\frac{1}{3}$ of the sites are in coincidence and $\Sigma 1$ means all sites are coincident. $\Sigma 1$ is often used to denote a low-angle boundary. Because of the ubiquitous role of grain boundaries in determining materials properties, efforts to model materials behavior require detailed information about the physical properties and distribution of grain boundaries. This information is also essential to engineer beneficial distributions of special grain boundary types by so-called "grain boundary engineering" [3,4].

Experimentally, grain boundary structures have been studied by diverse methods including, etch pit analysis, optical polarization microscopy, high-resolution TEM, and most recently electron backscattering diffraction (EBSD) [5-7]. EBSD measurements have been particularly powerful for developing a statistical understanding of grain boundary types. With EBSD measurements the misorientation of neighbor grains can be obtained by indexing the diffraction patterns of each grain and by categorizing the misorientation as consistent with or inconsistent with the predictions of a CSL model.

Although the grain boundary normal is believed to play an important role in energy minimization, whether or not a CSL exhibits special behavior depends principally on the orientation of the boundary plane [8], surface maps that identify neighbor-grain misorientation and the grain boundary intercept at the surface, leave 1 degree of freedom undetermined. As a result, surface-sensitive electron methods typically do not provide full grain-boundary-normal information. Electron-beam methods can sometimes be extended by serial sectioning or by TEM of highly inclined boundaries in foil samples, but there are very few examples of published CSL data that also report boundary normals. A true nondestructive three-dimensional (3D) probe is essential to provide detailed information about grain boundary structure and to correlate structural information with properties. This information will address long-standing fundamental issues of grain boundary structure and will connect directly to advanced modeling efforts.

2. 3D X-ray crystal microscopy

Here we report on X-ray microdiffraction characterization of grain boundary type with a recently commissioned 3D X-ray Crystal Microscope on beamline 34-ID at the Advanced Photon Source. This emerging experimental tool provides an unprecedented test of grain boundary structure with misorientation sensitivity more than an order of magnitude better than with EBSD ($<0.01^\circ$), and with nondestructive sensitivity to grain-boundary 3D morphology. Although it is slower than the 3D X-ray diffraction microscope developed by the RisØ and the European Synchrotron Radiation Facility (ESRF) [9-11], its higher spatial and angular resolution make it ideal for detailed characterization of grain boundaries. Key is the use of polychromatic radiation and differential aperture microscopy, which allows the single crystal diffraction from subgrain volumes within the sample to be probed [12,13]. Fig. 1 shows a schematic of the 3D X-ray Crystal Microscope. A pair of elliptical nondispersive total-external-reflection Kirkpatrick–Baez (K–B) mirrors focus an intense polychromatic X-ray beam to a $0.5\,\mu m \times 0.5\,\mu m$ spot on a sample [14]. The Laue patterns generated by volume elements (voxels) along the X-ray beam are collected by an X-ray CCD. The overlapping Laue patterns are decoded by a differential-aperture that scans across the surface of the sample [12]. By subtraction of CCD image pairs, which differ only by a small (differential) motion of a heavy Z wire near the sample, the source of the observed intensity in each pixel of the CCD detector can be assigned to length segments along the X-ray beam with $\sim 1\,\mu m$ resolution. The decoded Laue patterns, are used to determine the local crystallographic orientation, unit cell shape (deviatoric elastic strain tensor) and plastic deformation within each voxel. Additionally

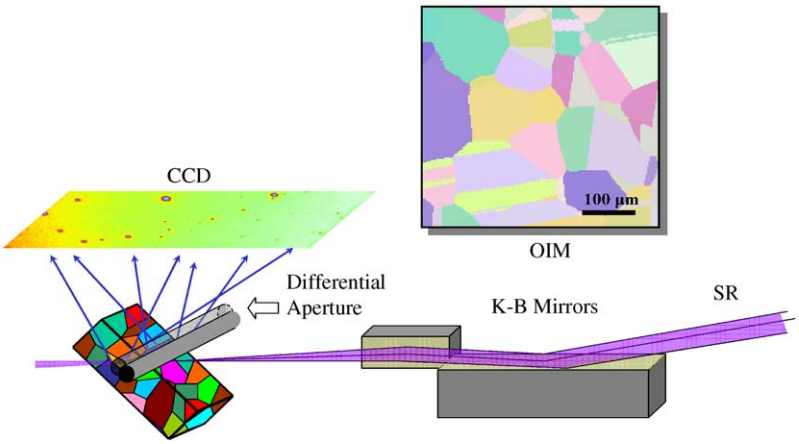

Fig. 1. Schematic of the 3D X-ray Crystal Microscope. The incident X-ray beam can be selected to have either a polychromatic or a monochromatic spectra. A 50 μm-diameter platinum wire is translated near the sample surface to decode the origin of the overlapping Laue patterns. The upper-right map shows a two-dimensional orientation imaging micrograph (OIM) of near-surface grains without depth profiling.

the full elastic strain tensor can be measured if the energy of at least one reflection is determined by inserting a scanning nondispersive monochromator into the incident beam [15].

3. Experimental

A recrystallized nickel polycrystalline sample was used to demonstrate the application of the 3D X-ray Crystal Microscope to grain boundary characterization. The experiments are straightforward as indicated in Fig. 2(a). The sample, has grains of about 50–150 μm with a face-centered cubic crystalline structure. The sample was surveyed, *without depth profiling,* to find the approximate locations of grain boundaries near the surface. The upper-right map in Fig. 1 shows a two-dimensional orientation map of the near-surface grains formed by X-ray microdiffraction from the sample. This mapping technique is quite similar to orientation imaging microscopy (OIM) of EBSD, but samples down about 50 μm below the surface [16]. Once a grain boundary is detected, three (four in practice) differential-aperture scans are made near the boundary to determine the location of the grain boundary at three linearly independent positions (Fig. 2(a)). Assuming a locally planar grain boundary, three X-ray beam/grain-boundary intersects define the plane normal and position. Of course as described below, full 3D surfaces can be measured to determine grain

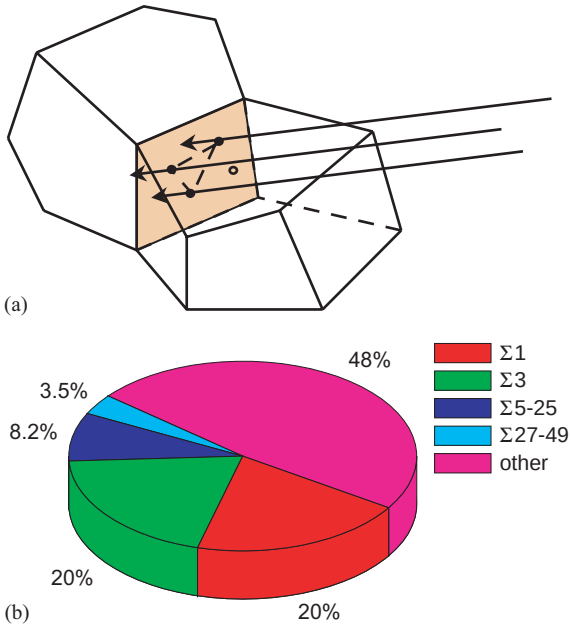

Fig. 2. (a) Once a grain boundary is selected, differential-aperture measurements, of typically 10 μm apart, are made to locate the grain boundary at three (four in practice) linearly independent positions. (b) The statistics of measured grain boundaries within the framework of CSL model.

boundary curvature, but these measurements are much slower and the application to a large number of grain boundaries will only be practical when faster detectors are available.

Analysis of 3D grain boundary data was made within the framework of the CSL model. First, Laue patterns were indexed to determine the precise orientation matrix of each grain. This analysis simultaneously determines the axis of rotation of one grain relative to another and the minimum rotation from all equivalent lattice orientations. The angle/axis pairs were categorized with respect to the nearest CSL type (Σ number) [17]. Additionally, the angle between the grain boundary normal and the misorientation axis was calculated. If the misorientation axis is parallel to the boundary normal, the boundary is a twist type; if the axis is in the boundary plane, then the boundary is a tilt type. Boundary crystallography can be classified as twist, symmetrical tilt, asymmetrical tilt, low-index, and irrational [5]. The proportion and distribution of these types eventually control the grain boundary network properties.

4. Results and discussion

The results of our CSL analysis are summarized in Fig. 2(b) and Table 1. From 85 measured grain boundaries that intersect the sample surface, about 52% are consistent with CSLs with Σ values up to 49. Each grain boundary was compared to a model CSL with the nearest Σ. The maximum allowed deviation, V_m, which corresponds to the highest density of dislocations possible in the boundary, is defined by the commonly used Brandon criterion:

$$V_m = V_0 \sum^{-1/2}.$$

Here $V_0 = 15^\circ$, is a constant of angular limit for low angle or $\Sigma = 1$ boundaries [18]. We also used the more restrictive Palumbo–Aust criterion, $V_m = V_0 \Sigma^{-5/6}$, to classify boundaries [19]; only 35% were found to be CSL boundaries. From the frequency distribution of CSLs, $\Sigma 1$ and $\Sigma 3$ boundaries are the dominant types observed. In general, low stacking fault energy results in twin boundaries that increase the $\Sigma 3$ proportion, and $\Sigma 1$ boundaries are related to preferred orientation where there is an increased probability for neighbor grains with almost the same orientation. Because of the high angular precision in these measurements it is possible to study small deviations from the CSL model with good confidence. We observe, for example, that the relative deviations of misorientation angle and axis from an ideal CSL model is very small for $\Sigma 3$s;

Table 1
The statistics and some typical CSLs of measured 85 grain boundaries

Sigma type	Σ1	Σ1	Σ3	Σ3	Σ7	Σ21b	Σ25b
Rotation axis (RAX)	−0.889, −0.444, −0.112	−0.277, 0.545, 0.791	−0.577, −0.577, 0.577	0.577, 0.577, −0.577	0.541, 0.637, −0.550	−0.439, −0.367, −0.820	0.684, 0.675, −0.277
Rotation angle (degree)	12.13	7.93	60.00	60.00	40.98	44.43	53.98
Rotation axis off (degree)	N/A	N/A	0.00	0.00	4.31	2.95	2.86
Rotation angle off (degree)	N/A	N/A	0.00	0.00	2.77	0.03	2.30
Boundary normals (BN) in bi-crystals	−0.01, 0.19, 0.98	−0.34, −0.82, 0.46	0.59, 0.79, 0.13	0.85, 0.22, −0.48	0.06, 0.84, −0.54	0.43, 0.27, 0.86	0.63, −0.68, 0.36
	0.08, 0.00, 1.00	−0.46, −0.79, 0.40	0.97, 0.25, −0.04	0.81, 0.55, −0.19	0.08, 0.60, −0.80	0.50, 0.28, 0.82	0.29, −0.10, 0.95
Angle between RAX and BN (degree)	79	89	43	26	30	6	83
Boundary plane type	Tilt	Tilt				Twist	Tilt
Statistics of total 85 boundaries: Σ1 = 20%, Σ3 = 20%, Σ5–25 = 8%, Σ27–49 = 4%.							

Rotation axis off and rotation angle off are the deviations of axis and angle from CSL model.

most of the measured misorientation angles and axes are within the small experimental uncertainty of the theoretical CSL values, with deviations of less than 0.03°. This result is consistent with the origin of Σ3 (twin) boundaries from within single grains as opposed to the origin of general grain boundaries from collisions of misoriented grains.

Table 1 lists some of the measured Σ boundaries, with misorientation axes, angles, deviations of axis and angle from CSL model, boundary plane normals, and boundary types. For the grain boundary normal, the uncertainty of measurement is mainly due to the limited spatial resolution of our differential aperture technique. Typically the normal can be determined to $\pm 0.5\,\mu m$ in $10\,\mu m$ or $\sim\pm 3^\circ$. Among all measured boundaries, about $<20\%$ are found to be tilt boundaries, twist boundaries or to have low-index planes in both grains. In general these boundary types are believed to have lower energies and less mismatch compared to irrational boundaries [2].

In grain boundary engineering, an important aspect is the adjustment of the proportion and distribution of certain CSLs to improve the collective behavior of polycrystals. Triple junctions with Σ1 and Σ3 boundaries are advantageous to reduce intergranular degradation; they suppress the network effect for transport phenomena. In Fig. 3, we illustrate how 3D X-ray diffraction microscopy can be applied to the study of triple junctions and how the simple local plane approximation applied above can be extended to the study of grain boundary curvature.

The 3D morphology of a triple junction was nondestructively mapped within a volume of about $26 \times 70 \times 50\,\mu m^3$. The transverse spatial resolution is about 1-2 μm, although it can be improved to 0.5 μm by using smaller step size. Fig. 3(a) shows the morphology of the triple junction and 3(b) shows the sample's surface contour. In Fig. 3(b), a ~10 μm surface step between grains is observed. Two of all three grain-boundaries are identified as low angle (Σ1) boundaries. By checking the misorientations near the boundaries, no observable local variation was found at angular sensitivity of 0.01° for this recrystallized nickel polycrystalline sample.

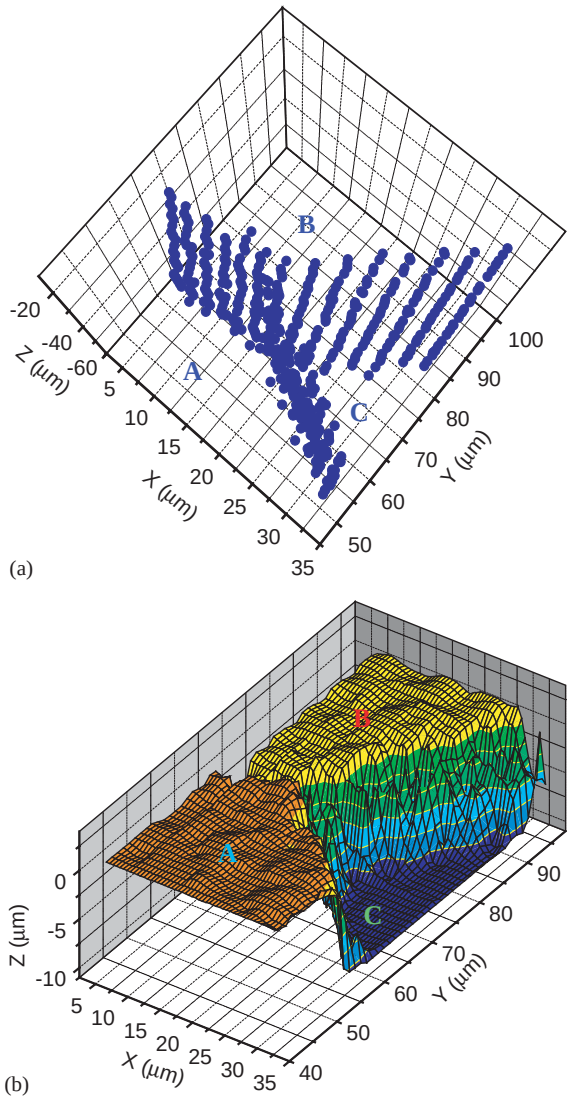

Fig. 3. The three-dimensional morphology of a triple junction was mapped by X-ray crystal microscopy. (a) Boundary surfaces. The misorientation angles between neighbor grains are 5.538° (C–A), 12.907° (B–C), and 16.572° (A–B), respectively. (b) Surface contour around the triple junction.

5. Conclusions

We have demonstrated the potential of 3D X-ray crystal microscopy to study the grain boundary network in materials. The ability to make high-precision measurements of grain boundary type

opens up a number of intriguing questions for the future. For example, how do grain boundary structures deviate from coincident site lattice models? Similarly, what is the distribution of grain boundary normals for a given Σ and how do variations in the normals effect grain boundary properties? Furthermore, how is the grain boundary distribution effected by intersection with a free surface? Finally, of particular interest will be measurements of grain boundary evolution during processing.

In order to answer the questions above, improved statistical information will be needed. Fortunately our measurements are only a first step in what will evolve to be an important new characterization tool of grain boundary type and our ability to improve the statistical information is increasing rapidly. The scope and detail of measurements will improve with better area detectors and smaller X-ray beams. X-ray microbeam spot size, detector spatial resolution, dynamic range and readout speed are all anticipated to improve by orders-of-magnitude over the next few years. In particular, commercial detectors are now available that will accelerate these measurements by a factor of >10, and new differential aperture methods promise an addition factor of 10 reduced data collection time. These developments will allow for vastly better statistical information, for improved spatial resolution leading to more accurate determination of grain-boundary surface morphology and for measurements on grains an order of magnitude smaller than are now possible.

Acknowledgements

We wish to thank Amit Goyal for the sample and for helpful suggestions on the manuscript. Work sponsored by the office of Basic Energy Science, Division of Materials Sciences and Engineering through the Oak Ridge National Laboratory, which is operated by UT-Battelle, LLC, for the US Department of Energy under contract DE-AC05-00OR22725. Work in part on Unicat beamline 34-ID at the Advanced Photon Source (APS). The APS is supported by the US DOE, Basic Energy Sciences, Office of Science under contract No. W-31-109-ENG-38.

References

[1] M.L. Kronberg, F.H. Wilson, Met. Trans. 185 (1949) 501.
[2] V. Randle, The Role of the Coincidence Site Lattice in Grain Boundary Engineering, The University Press, Cambridge, 1996.
[3] T. Watanabe, Res. Mech. 11 (1984) 47.
[4] G. Palumbo, K.T. Aust, in: D. Wolf, S. Yip (Eds.), Materials Interfaces: Atomic Level Structure and Properties, Chapman and Hall, London, 1992 Chapter 5.
[5] V. Randle, The Measurement of Grain boundary Geometry, Institute of Physics Pub., Bristol, UK, 1993.
[6] A. Berger, P.J. Wilbrandt, P. Haasen, Acta Metall 31 (1983) 1443.
[7] F.J. Humphreys, J. Mater. Sci. 36 (2001) 3833.
[8] V. Randle, H. Davies, Ultramicroscopy 90 (2002) 153.
[9] H.F. Poulsen, S.F. Nielsen, E.M. Lauridsen, S. Schmidt, R.M. Suter, U. Lienert, L. Margulies, T. Lorentzen, D. Juul Jensen, J. Appl. Crystallogr. 34 (2001) 751.
[10] X. Fu, H.F. Poulsen, S. Schmidt, S.F. Nielsen, E.M. Lauridsen, D. Juul Jensen, Scripta Mater. 49 (2003) 1093.
[11] H.F. Poulsen, S. Schmidt, J. Appl. Crystallogr 36 (2003) 319.
[12] B.C. Larson, W. Yang, G.E. Ice, J.D. Budai, J.Z. Tischler, Nature 415 (2002) 887.
[13] J.S. Chung, G.E. Ice, J. Appl. Phys. 86 (1999) 5249.
[14] G.E. Ice, J.S. Chung, J.Z. Tischler, A. Lunt, L. Assoufid, Rev. Sci. Institute 71 (2000) 2635.
[15] G.E. Ice, J.S. Chung, W. Lowe, E. Williams, J. Edelman, Rev. Sci. Institute 71 (2000) 2001.
[16] J.D. Budai, W. Yang, N. Tamura, J. -S. Chung, J.Z. Tischler, B.C. Larson, G.E. Ice, C. Park, D.P. Norton, Nat. Mater. 2 (2003) 487.
[17] H. Mykura, Grain Boundary Structure and Kinetics, ASM, OH, USA, 1980.
[18] D.G. Brandon, Acta Metall 14 (1966) 1479.
[19] G. Palumbo, K.T. Aust, E.M. Lehockey, U. Erb, P. Lin, Scripta Mater. 38 (1998) 1685.